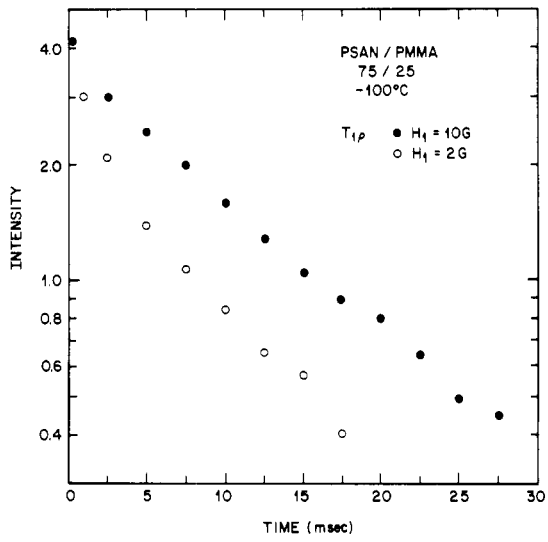

Figure 4. $T_{1\rho}$ decay for 75/25 PSAN/PMMA for H_1 = 10 and 2 G, respectively.

low-temperature minimum, Figure 3 shows that $(7.1 + \omega_1)k$ does not vary linearly with ω_1; the relaxation rate for the blends falls short of the magnitudes expected from a tightly coupled spin system. In this case, however, a diffusive path length of only about 17 Å would be required to eliminate spin diffusion as a rate-controlling step. These data therefore indicate that there is segregation on a scale between 20 and 150 Å.

The question now arises as to why simple exponential $T_{1\rho}$ decay is observed at $H_1 \approx 10$ g in most samples. One would expect nonexponential behavior for a segregated system with the overriding caveat that it is not possible to resolve two $T_{1\rho}$ components which are within a factor of 2, using only the 1.5 decades of decay observable with our system. In this context the marginally nonexponential decay observed in the 75/25 PSAN/PMMA blend alluded to in the earlier part of this section assumes critical significance. If nonexponential decay is to be observed at all, the 75/25 blend is the obvious candidate since there is greatest chance of having some of the PSAN material remote from the dilute PMMA. Furthermore, the curvature in the decay should increase at lower H_1 fields since $T_{1\rho}$ will decrease without altering the diffusive path length. Data recorded at H_1 = 7.3G and 2.0 G at -100 °C are listed in Table I. The nonexponential character of the $T_{1\rho}$ decays unambiguously increases as required to be consistent with component polymer segregation. Figure 4 compares the $T_{1\rho}$ decay for H_1 = 2 and 10 G in the 75/25 PSAN/PMMA material.

In summary, the NMR data presented in this paper indicate that there is inhomogeneity on a scale between 20 and 150 Å, determined by the experiment, in the PSAN/PMMA blends studied.

References and Notes

(1) K. Naito, G. E. Johnson, D. L. Allara, and T. K. Kwei, *Macromolecules*, preceding paper in this issue.
(2) J. G. Powles and P. Mansfield, *Phys. Lett.*, **2**, 58, (1962).
(3) H. Y. Cano and E. M. Purcell, *Phys. Rev.*, **94**, 630 (1954).
(4) S. R. Hartmann and E. L. Hahn, *Phys. Rev.*, **128**, 2042 (1962).
(5) G. P. Jones, D. C. Douglass, and D. W. McCall, *Rev. Sci. Instrum.*, **36**, 1461 (1965).
(6) D. W. McCall, *Natl. Bur. Stand. (U.S.), Spec. Publ.*, **No. 310**, 475 (1969).
(7) D. C. Douglass and V. J. McBrierty, *J. Chem. Phys.*, **54**, 4085 (1971).
(8) R. A. Assink and G. L. Wilkes, *J. Polym. Eng. Sci.*, **17**, 606 (1977).
(9) G. E. Wardell, V. J. McBrierty, and D. C. Douglass, *J. Appl. Phys.*, **45**, 3441 (1974).
(10) N. Bloembergen, *Physica (The Hague)*, **15**, 386 (1949).

Interaction Parameter in Polymer Mixtures

T. K. Kwei* and H. L. Frisch†

Bell Laboratories, Murray Hill, New Jersey 07974. *Received June 27, 1978*

ABSTRACT: An improved method has been devised to calculate, from melting point measurements, the interaction parameter between a crystalline and an amorphous polymer. The procedure takes into account the effect of morphological changes in melting point depression.

The determination of thermodynamic interaction between two polymers is crucial to the understanding of compatibility in mixtures. Of the several methods which have been applied recently to amorphous polymers, namely, small-angle neutron scattering,[1] gas–liquid (polymer) chromatography,[2–4] and vapor sorption,[5] none is readily adaptable to a mixture containing a crystalline polymer as one of its components. Nishi and Wang,[6] in their analysis of the lowering of the melting temperature of a crystalline polymer in the presence of an amorphous one, derived a simple equation which related the melting point depression directly to the interaction parameter. Their equation described satisfactorily the data obtained for mixtures of poly(vinylidene fluoride) and poly(methyl methacrylate)[6] or poly(ethyl methacrylate).[7]

From a study of isothermally crystallized samples, Nishi and Wang concluded that morphological changes such as imperfections in crystals and reduction in lamellar thickness were not major factors in the lowering of the melting point in a PVF_2–PMMA mixture. Nevertheless, it is worthwhile to examine the possibility that such morphological contributions may be important in other blends. A case in point is the mixture of poly(2,6-dimethyl-1,4-phenylene oxide) (PPO) and isotactic polystyrene (PS) for which a reduction in the thickness of i-PS crystals has been indicated by small-angle X-ray studies.[8] In the present investigation, we have extended the treatment of Nishi and Wang to take morphological effects into account. A procedure has been devised so that both the interaction parameter and the morphological contribution can be calculated from melting point measurements.

The interaction parameter between PPO and PS has been determined by melting point measurements in two previous investigations. Shultz and McCullough[9] used ternary mixtures of PPO–PS–toluene and Berghmans and Overbergh[10] used isotactic PS and PPO. In both studies, the interaction parameter was found to be approximately

† Department of Chemistry, State University of New York at Albany, Albany, New York 12222.

0024-9297/78/2211-1267$01.00/0

zero but morphological effects were not considered specifically. We have employed mixtures of crystalline PPO and amorphous PS. As it turned out, the procedure we adopted for preparing samples amplified the importance of morphological effects and thus provided a convenient means for assessing their magnitude.

Melting Point Equation

In the following derivation the crystallizable polymer will be designated component 2 and the amorphous polymer, component 1. The free-energy difference per segment between the crystal and the supercooled liquid is

$$\Delta F(T,\zeta) = F(T,\zeta) - F_a(T,\phi_1) \quad (1)$$

where ζ is the number of segments between the two lamellar surfaces of a crystal, the subscript a indicates the amorphous liquid state, and ϕ_1 is the volume fraction of component 1 in the liquid. Equation 1 can be rewritten as

$$\Delta F(T,\zeta) = [F(T,\zeta) - F(T,\zeta^0)] + [F(T,\zeta^0) - F_a(T,\phi_1 = 0)] + [F_a(T,\phi_1 = 0) - F_a(T,\phi_1)] \quad (2)$$

The superscript 0 in eq 2 refers to component 2 crystallized in the absence of component 1, i.e., our reference material. The three bracketed terms on the right-hand side of eq 2 represent respectively the free-energy changes due to morphological effects, fusion, and mixing. Each of these terms is given by a standard thermodynamic expression:

$$F(T,\zeta) - F(T,\zeta^0) = (2\sigma_e/\zeta) - (2\sigma_e/\zeta)^0 \quad (3)$$

$$F(T,\zeta^0) - F_a(T,\phi_1 = 0) = -\Delta H_u(T_m^0 - T_m)/T_m^0 \quad (4)$$

$$F_a(T,\phi_1 = 0) - F_a(T,\phi_1) = \frac{RT}{m_2}[\ln \phi_2 + \phi_1 - \phi_1 m_2/m_1 + \chi_{21}\phi_1^2] \quad (5)$$

The surface free energy $2\sigma_e$ per stem of segments in a lamella is defined here in a broad sense to include the contribution from surface-induced defects. The interaction parameter χ and the chain lengths m_1 and m_2 are linked by the relation

$$\chi_{21}' = \chi_{21}/m_2 = \chi_{12}/m_1 \quad (6)$$

Upon setting $\Delta F(T,\zeta) = 0$ at the melting point T_m, we obtain, by combining eq 2 to 4 and by expanding $\ln \phi_2$ in a series, eq 7:

$$\Delta H_u(T_m^0 - T_m)/T_m^0 = [(2\sigma_e/\zeta) - (2\sigma_e/\zeta)^0] + RT_m[\phi_1/m_1 - (\chi_{21}' - \tfrac{1}{2}m_2)\phi_1^2 + \phi_1^3/3m_2 + \ldots] \quad (7)$$

If $[(2\sigma_e/\zeta) - (2\sigma_e/\zeta)^0] = 0$ and m_2 is very large, eq 7 reduces to Flory's expression:

$$(1/T_m - 1/T_m^0) = R(\phi_1 - \chi_{12}\phi_1^2)/m_1\Delta H_u \quad (8)$$

When m_1 is also very large, the equation is further simplified to that derived by Nishi and Wang.

$$(1/T_m - 1/T_m^0) = -R\chi_{21}'\phi_1^2/\Delta H_u \quad (9)$$

The term $[(2\sigma_e/\zeta) - (2\sigma_e/\zeta)^0]$ is obviously a function of ϕ_1 and vanishes at $\phi_1 = 0$. We assume, as a first approximation, that the quantity is proportional to ϕ_1, with a proportionality constant C. The justification for this assumption is found in the study of i-PS–PPO mixtures for which the crystallite thickness decreases almost linearly with increasing amounts of the noncrystalline component. Therefore, we write $\zeta = \zeta^0(1 - q\phi_1)$ and

$$(2\sigma_e/\zeta) - (2\sigma_e/\zeta)^0 \approx (2\sigma_e/\zeta)^0 q\phi_1 \quad (10)$$

for $\sigma_e \approx \sigma_e^0$ and $q \ll 1$.

If we further assume that the temperature dependence of χ is given by the usual expression $\chi = a + b/T$ and that $a \ll b/T$ near the melting point of PPO, the final equation becomes:

$$\Delta H_u(T_m^0 - T_m)/\phi_1 RT_m^0 - T_m/m_1 - \phi_1 T_m/2m_2 = C/R - b\phi_1 \quad (11)$$

A plot of the left-hand side of eq 11 vs. ϕ_1 would then yield a straight line with a slope of $-b$ and an intercept of C/R. At first glance, eq 11 may seem unnecessarily complicated, but, as we shall see later, the terms containing m_1 and m_2 cannot be omitted for the polymers used in our study.

Experimental Section

Materials. Poly(2,6-dimethyl-1,4-phenylene oxide) was obtained through the courtesy of Dr. A. Katchman of General Electric Co. It was purified by precipitating a 5% toluene solution into a large volume of methanol. The powdery precipitate was dried under vacuum at 100 °C for 16 h. The molecular weight of the purified PPO was determined by gel permeation chromatography, using tetrahydrofuran as solvent. When compared to polystyrene standards, the molecular weights of PPO were calculated to be: $\bar{M}_n = 1.10 \times 10^4$, $\bar{M}_w = 4.35 \times 10^4$, and $\bar{M}_z = 9.72 \times 10^4$. The density of PPO was 1.066 at 25 °C.[12]

Four monodisperse polystyrene samples were procured from Pressure Chemicals Co. The molecular weights of these samples were given by the supplier as 800 ($M_w/M_n < 1.3$), 2200 ($M_w/M_n < 1.06$), 10000 ($M_w/M_n < 1.06$), and 37000 ($M_w/M_n < 1.06$). Films of these samples were pressed from the melt and the densities of the films were determined in a density gradient column to be 1.030, 1.039, 1.043, and 1.044 g cm^{-3}, respectively.

Sample Preparation. The purified PPO powder had a very low degree of crystallinity. But crystallization took place when a 20-mL aliquot of a 2% toluene solution was allowed to evaporate slowly at room temperature over a period of 3 to 4 days. The resulting material exhibited a measurable heat of fusion. Hence, all specimens were prepared from toluene solution in accordance with the above procedure. The thickness of the resulting specimen, which was usually fragile (powdery in the case of crystallized PPO), was approximately 0.01 cm.

In the course of our calorimetric study, the importance of a suitable drying temperature was soon impressed on us. Drying at temperatures below T_g was often ineffective in the removal of toluene and resulted in low T_m and T_g values. On the other hand, an excessively high drying temperature caused partial melting of PPO crystals and led to erroneous values of heat of fusion. For these reasons, all specimens were dried in two steps. They were first placed in a vacuum oven at 100 °C for 16 h. Calorimetric measurements were then made for each sample. After examining the thermograms, we redried each new specimen at a temperature chosen to be 35 °C below the inception of melting. But in no case did the drying temperature exceed 160 °C in order to avoid thermal degradation of the polymers. We found that consistent calorimetric results could be obtained with the redried samples. However, there were a few exceptions. When the weight fraction of PPO in the blend was high and the glass transition of the mixture occurred near the beginning of the fusion process, we were unable to find a proper condition for redrying.

Although PPO has a high glass transition temperature, drying at 100 °C was apparently effective in the removal of toluene as the T_m and T_g values agreed well with literature data.[13,14]

Calorimetry. A DuPont thermal analyzer, Model 990, with a DSC cell was used. A typical sample weight was between 10 and 15 mg. A heating rate of 10 °C/min was employed throughout our study, but two additional experiments were carried out at 5 °C/min for the purpose of comparison. At the conclusion of a DSC experiment, the sample was cooled in the cell at a rate of 50 °C/min. The thermal scan was then repeated for the quenched sample.

The temperature (extrapolated) of initial rise in C_p in the glass transition region was taken as T_g while the final temperature (also extrapolated) of the melting endotherm was identified as T_m. The reproducibility of T_g or T_m measurements was about ±0.5 °C.

Table I
Thermal Transitions of PS(1)-PPO(2) Mixtures

component 1	W_1	as cast T_g, °C	as cast T_m, °C	as cast Q/Q_0	quenched T_g, °C
none	0		262	1.00	212
	0		260[a]	0.98[a]	211
PS 800	1.000				6
	0.909	9	163	0.10	12
	0.800	14	170	0.24	24
	0.500	40	197	0.53	59
	0.333	72	215	0.65	98
	0.167	112	237	0.82	148
PS 2200	1.000				54
	0.909	61[b]	182	0.093	61
	0.800	69[b]	189	0.23	70
	0.500	88	214	0.55	104
	0.500	87[a]	212[a]	0.48[a]	103[a]
	0.333	119	229	0.69	131
PS 10000	1.000				92
	0.909	96	210	0.11	97
	0.800	102[b]	217	0.26	105
	0.667	116[b]	224	0.37	116
	0.588	121	228	0.41	125
	0.500	130	233	0.46	135
	0.412	141	238	0.51	144
PS 37000	1.000				100
	0.833	110[b]	224	0.10	110
	0.800	108[b]	226	0.21	112
	0.667	117	231	0.28	123
	0.500	119	239	0.49	139

[a] Heating rate 5 °C/min. [b] Enthalpy relaxation.

Samples prepared at different times showed somewhat larger variation in T_m, about ±1.0 °C. The data presented in this paper are the averages of duplicate or triplicate measurements.

Results

The thermogram of purified PPO powder showed a T_g at 205 °C and a small melting endotherm between 230 and 254 °C. For the sample crystallized from toluene, the glass transition could not be identified in the thermogram, but the heat of fusion was about 4 cal/g. The melting endotherm was very broad and had a span of about 60 °C between the inception and the end of the fusion process. The final melting point was 262 °C, in excellent agreement with literature data.[13,14] After the fusion process was completed and the sample was quenched from the melt, crystallinity was completely lost. The quenched sample had a T_g of 212 °C, again in good agreement with literature values.[12,14]

In the C_p curves for the four polystyrene samples, enthalpy relaxation effects were pronounced. These effects, however, were eliminated almost completely in quenched samples.

For the PS–PPO mixtures, each thermogram showed a glass transition and a melting endotherm. After quenching, all mixtures became amorphous, and each of them showed a well-defined T_g.

The calorimetric results are summarized in Table I, in which the fifth column lists the ratios of the heats of fusion, Q, of the mixtures to the corresponding value Q_0 for PPO. The uncertainty in matching base lines before and after melting introduces an error of about 5 to 10% in the values of Q/Q_0. The melting temperatures of the blends are plotted against compositions in Figure 1. Similarly, the glass transition temperatures of the quenched specimens are displayed in Figure 2. The ratio Q/Q_0 is proportional to the weight fraction of PPO in the blend, as shown in Figure 3.

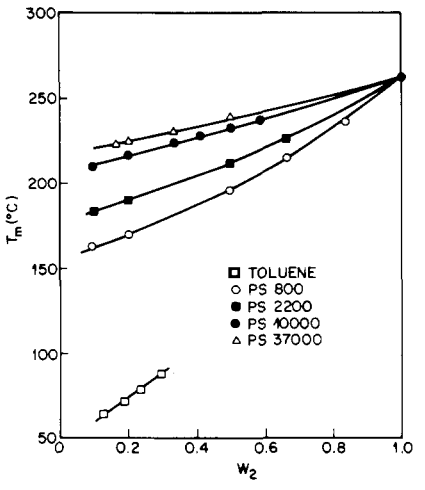

Figure 1. Melting temperatures of PPO–PS mixtures. Data for toluene from ref 9.

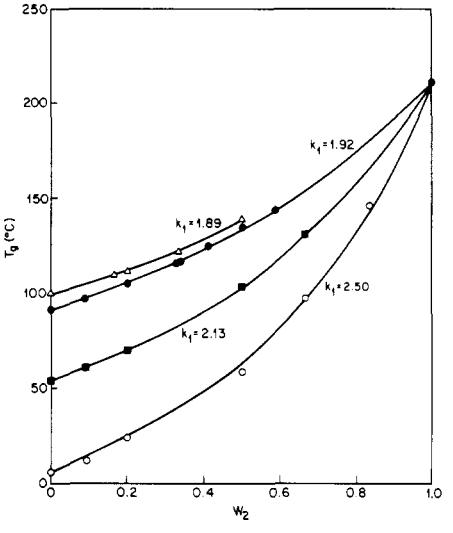

Figure 2. Glass transition temperatures of quenched PPO–PS mixtures. Solid curves represent calculated values.

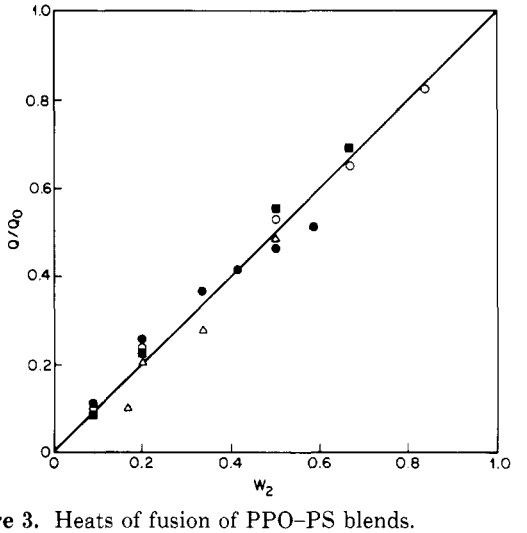

Figure 3. Heats of fusion of PPO–PS blends.

Discussion

1. Glass Transition. The glass transition temperatures of the quenched blends can be represented by an equation of the type used by Wood[15] or by Gordon and Taylor.[16]

$$T_g = (k_1 w_1 T_{g1} + w_2 T_{g2}) / (k_1 w_1 + w_2) \qquad (12)$$

In eq 12, w denotes weight fraction and k_1 is a constant

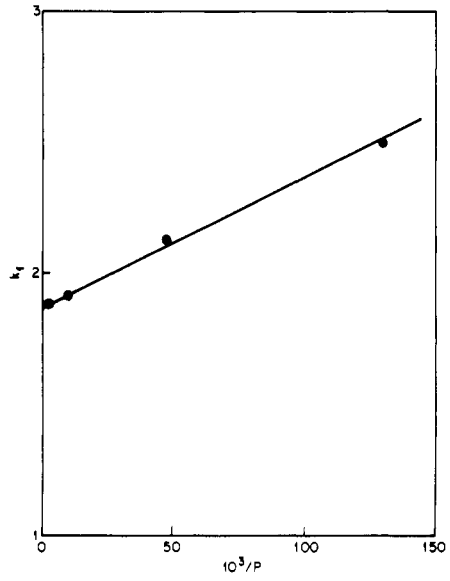

Figure 4. Effect of PS molecular weight on k_1.

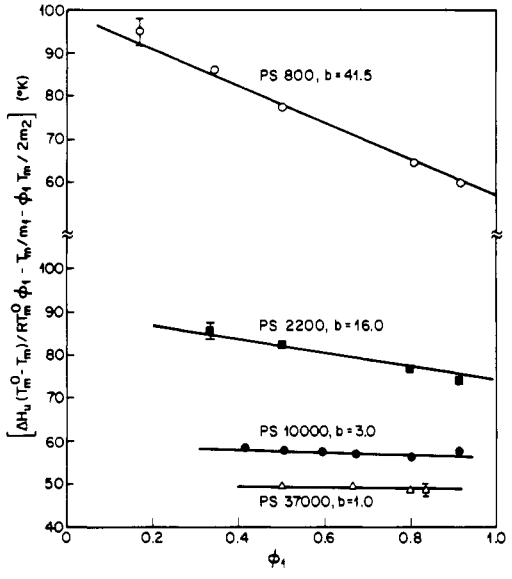

Figure 5. Melting point data plotted according to eq 11.

characteristic of the polymer pair. The k_1 values are indicated in Figure 2 for the four fitted curves. Agreement between calculated and experimental T_g values is within 1 °C for mixtures containing PS 37 000, 10 000, and 2 200; it is less striking in the case of PS 800, the largest discrepancy being 5 °C. Since the densities of PPO and PS differ by only a few percent, an alternative equation using volume fraction[17] also gives a good fit of the experimental data.

In comparing our results with literature data, we find that the value of $1/k_1$ for PS 37 000 is smaller than that obtained by Fried, Karasz, and MacKnight.[12] The discrepancy may arise, in part, from the different procedures used to identify T_g. These authors used the end of the C_p increase as T_g while we used the beginning.

We note that the k_1 values always exceeded unity. If the free volume theory is taken literally, then we may conclude that PS is more effective than PPO in its contribution to the free volume of the mixture. The free volume theory also provides a rational basis for understanding the dependence of k_1 on the degree of polymerization, P, of PS. We consider k_1 as being composed of contributions from the chain ends, k_e, and from internal segments, k_i. Therefore k_1 may be written as

$$k_1 = k_i + 2(k_e - k_i)/P \qquad (13)$$

A linear relation between k_1 and the reciprocal of PS molecular weight is predicted by eq 13 and indeed it describes our results exceedingly well (Figure 4). We obtain, from the straight line, $k_i = 1.87$ and $k_e = 4.37$. As expected, k_e is larger than k_i, and the ratio $k_e/k_i \sim 2.3$ seems to be reasonable in magnitude.

2. Heat of Fusion. As we have already stated, the ratio Q/Q_0 is directly proportional to the weight fraction of PPO in the blend. Apparently, the ability of PPO to crystallize was not impeded by PS under the conditions of sample preparation employed in this investigation. The same relation was found for PVF_2–PMMA mixtures.[6]

3. Melting Temperatures. When the melting point data for each set of PS–PPO mixtures were plotted as $\Delta H_u(1/T_m - 1/T_m^0)/R\phi_1$ vs. ϕ_1, in accordance with eq 8, the intercept did not equal $1/m_1$. This was in sharp contrast with PVF_2–PMMA or PVF_2–PEMA mixtures, for which $1/m_1 \approx 0$ and the corresponding plots yielded near-zero intercepts. Therefore, we decided from the outset that the morphological term C should be included in the treatment of our data. In calculating the three terms on the left-hand side of eq 11, we have used $\Delta H_u = 10.1$ cal/g,[9,18] $m_2 = 91$, and $m_1 = \bar{V}_1/v_{2u}$ where $\bar{V}_1$ is the molar volume of PS and v_{2u} that of a PPO segment. The resulting plots are shown in Figure 5. The parameters C and b obtained from the intercept and the slope of each linear plot are compiled in Table II. The magnitude of the constant b decreases from 41.5 for PS 800 to 1.0 for PS 37 000. The value of χ calculated from b/T for each PS–PPO pair is always less than the critical value of χ computed from the molecular weights of that pair (Table II). Therefore we believe our experimental findings to be internally consistent. However, it is likely that b will decrease in magnitude at lower temperatures in order not to violate the criterion of miscibility, i.e., $\chi < \chi_{cr}$. This possibility finds tentative support in the work of Weeks, Karasz, and MacKnight[19] who have found a small but negative enthalpy of mixing of the two polymers near room temperature. A second possibility is that the term a in $\chi = a + b/T$ is slightly negative and its contribution becomes significant at low temperatures.

Table II
Interaction Parameters and Morphological Effects in PS-PPO Mixtures[d]

	temp range, °C	b	χ	χ_{cr}[c]	C
PS 800	164-237	41.5	0.095-0.081	0.096	196.7
PS 2200	182-229	16.0	0.035-0.032	0.042	178.8
PS 10 000	200-238	3.0	0.0063-0.0059	0.010	117.2
PS 37 000	223-239	1.0	0.0020-0.0019	0.006	98.4
PS 78 000[a]	60-101		0		
i-PS + a-PPO[b]	~200		0		

[a] Reference 9. [b] Reference 10. [c] $2\chi_{cr} = ([1/m_{w_1}] + [m_{z_2}^{1/2}/m_{w_2}m_{z_1}^{1/2}]) + ([1/m_{w_2}] + [m_{z_1}^{1/2}/m_{w_1}m_{z_2}^{1/2}])$. We assume $m_{w_1} = m_{z_1}$ from $2\chi_{sp} = (\phi_1 m_{w_1})^{-1} + (\phi_2 m_{w_2})^{-1}$ and $\phi_{1c} = 1/[1 + (m_{w_1}m_{z_2}^{1/2})/(m_{w_2}m_{z_1}^{1/2})]$. [d] See ref 21 and 22.

The parameter b is also found to be inversely proportional to the chain length of PS (Figure 6). Since $b = B_{21}v_{2u}/R$, where B_{21} is the pair interaction energy per unit volume, this correlation dictates that B_{21} decreases as the chain length of PS increases. A logical explanation which we can offer at this time invokes the same kind of reasoning previously used for k_1. It seems that the contribution of the internal segments of PS to B or χ is zero in this case and that the chain ends are totally responsible

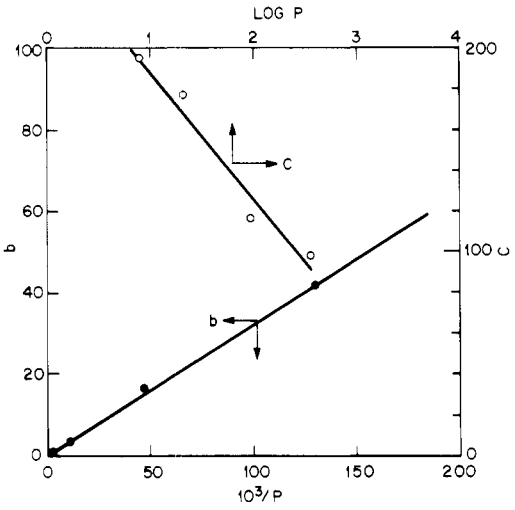

Figure 6. Effect of PS molecular weight on interaction parameter and morphological contribution.

for the magnitude of b. The vanishing value of χ for very high molecular weight PS agrees with the results of ref 9 and 10.

We now address the significance of the parameter C. In computing the various terms in eq 11, we have found that the morphological effect exceeds the free energy of mixing by a substantial margin in all cases. Although C decreases with increasing molecular weight of PS, so does b. Thus, the importance of the morphological term becomes more pronounced as molecular weight increases. When the molecular weight of PS reaches 37 000, the melting point depression is almost entirely attributable to morphological effects.

It remains to be shown that the magnitude of C calculated by us is consistent with reasonable values of σ_e, ζ^0, and ζ. For this purpose we have carried out the following computation using: $\sigma_e = 89$ erg cm^{-2} equal to the value for polyethylene,[20] ~ 40 Å^2 as the cross-sectional area of a PPO segment, and $\zeta^0 = 25$ segments. Thus, $2\sigma_e/\zeta^0$ is estimated to be 410 cal mol^{-1}. If ζ is reduced from 25 to 20, $[2\sigma_e/\zeta - (2\sigma_e/\zeta)^0] = 102$; for $\zeta = 17$, the latter quantity becomes 193. Therefore, modest changes in crystal thickness suffice to account for our C values.

At present, we do not understand fully the dependence of C on molecular weight. But we notice in passing an approximately linear relationship between C and log P (Figure 6).

Conclusion

We have devised a procedure to calculate, from melting point measurements, the interaction parameter between a crystalline and an amorphous polymer. The procedure takes into account the effect of morphological changes on melting point depression. The calculated values of χ for PPO–PS agree with earlier findings. The morphological contributions obtained from our analysis also seem to be reasonable in magnitude.

Acknowledgment. The authors wish to thank Mrs. M. Y. Hellman for molecular weight determinations. Encouraging discussions with Drs. E. Helfand and S. Matsuoka are gratefully acknowledged. One of us is indebted to the National Science Foundation for support of this research.

References and Notes

(1) W. A. Kruse, R. G. Kirste, J. Haas, B. J. Schmitt, and D. J. Stein, *Makromol. Chem.*, **177**, 1145 (1976).
(2) O. Olabisi, *Macromolecules*, **8**, 316 (1975).
(3) C. S. Su and D. Patterson, *Macromolecules*, **10**, 708 (1977).
(4) D. D. Desphande, D. Patterson, H. P. Schreiber, and C. S. Su, *Macromolecules*, **7**, 530 (1974).
(5) T. K. Kwei, T. Nishi, and R. F. Roberts, *Macromolecules*, **7**, 667 (1974).
(6) T. Nishi and T. T. Wang, *Macromolecules*, **8**, 909 (1975).
(7) T. K. Kwei, G. D. Patterson, and T. T. Wang, *Macromolecules*, **9**, 780 (1976).
(8) W. Wenig, F. E. Karasz, and W. J. MacKnight, *J. Appl. Phys.*, **46**, 4194 (1975).
(9) A. R. Shultz and C. R. McCullough, *J. Polymn. Sci., Part A-2*, **10**, 307 (1972).
(10) H. Berghmans and N. Overbergh, *J. Polym. Sci., Part A-2*, **15**, 1757 (1977).
(11) P. J. Flory, "Principles of Polymer Chemistry", Cornell University Press, Ithaca, N.Y., 1953, p 569.
(12) J. R. Fried, F. E. Karasz, and W. J. MacKnight, *Macromolecules*, **11**, 150 (1978).
(13) F. E. Karasz and J. M. O'Reilly, *J. Polym. Sci., Part B*, **3**, 561 (1965).
(14) F. E. Karasz, H. E. Bair, and J. M. O'Reilly, *J. Polym. Sci., Part A-2*, 6, 1141 (1968).
(15) L. A. Wood, *J. Polym. Sci.*, **28**, 319 (1958).
(16) M. Gordon and J. S. Taylor, *J. Appl. Chem.*, **2**, 495 (1952).
(17) F. N. Kelley and F. Bueche, *J. Polym. Sci.*, **50**, 549 (1961).
(18) F. E. Karasz, J. M. O'Reilly, H. E. Bair, and R. A. Kluge, *Polym. Prepr., Am. Chem. Soc., Div. Polym. Chem.*, **9**, 822 (1968).
(19) N. E. Weeks, F. E. Karasz, and W. J. MacKnight, *J. Appl. Phys.*, 48, 4068 (1977).
(20) H. E. Bair, T. N. Huseby, and R. Salovey, "Analytical Calorimetry", Plenum Press, New York, 1968, p 31.
(21) W. H. Stockmayer, *J. Chem. Phys.*, **17**, 588 (1949).
(22) H. A. G. Chernin and R. Koningsveld, *Macromolecules*, **2**, 207 (1969).

Metal Complexes of Poly(α-amino acids). Conformational Aspects of the Interaction between Cupric Ions and Poly(L-histidine)[1]

M. Palumbo, A. Cosani, M. Terbojevich, and E. Peggion*

Biopolymer Research Center of C.N.R., Institute of Organic Chemistry, University of Padova, 35100 Padova, Italy. *Received April 12, 1978*

ABSTRACT: The interaction between cupric ions and poly(L-histidine) under various experimental conditions has been investigated by potentiometric, visible absorption, and circular dichroism techniques. In addition to the low- and high-pH forms described by Levitzki et al.[2] a new complex has been detected, which is formed with poly(L-histidine) in the ordered structure. Moreover, at very low Cu/peptide ratios, a species is observed, the optical rotatory properties of which are time dependent and slowly transform into the CD pattern typical of the low-pH complex. From the spectroscopic properties, a structure has been proposed for the new complexes.

In 1967 Pecht and co-workers first reported that copper complexes of poly(L-histidine) [(L-His)$_n$] exhibit oxidase activity which is about two orders of magnitude higher than that of the Cu(II) aquo complex.[3] In a subsequent work investigations have been carried out in the attempt to correlate catalytic activity with stereochemistry of the

0024-9297/78/2211-1271$01.00/0